J Comp Physiol B (2012) 182:91–100
DOI 10.1007/s00360-011-0599-6

ORIGINAL PAPER

A radical approach to beating hypoxia: depressed free radical release from heart fibres of the hypoxia-tolerant epaulette shark (*Hemiscyllum ocellatum*)

Anthony J. R. Hickey · Gillian M. C. Renshaw · Ben Speers-Roesch · Jeffrey G. Richards · Yuxiang Wang · Anthony P. Farrell · Colin J. Brauner

Received: 6 February 2011 / Revised: 13 June 2011 / Accepted: 16 June 2011 / Published online: 12 July 2011

Abstract Hypoxia and warm ischemia are primary concerns in ischemic heart disease and transplant and trauma. Hypoxia impacts tissue ATP supply and can induce mitochondrial dysfunction that elevates reactive species release. The epaulette shark, *Hemiscyllum ocellatum*, is remarkably tolerant of severe hypoxia at temperatures up to 34°C, and therefore provides a valuable model to study warm hypoxia tolerance. Mitochondrial function was tested in saponin permeabilised ventricle fibres using high-resolution respirometry coupled with purpose-built fluorospectrometers. Ventricular mitochondrial function, stability and reactive species production of the epaulette shark was compared with that of the hypoxia-sensitive shovelnose ray, *Aptychotrema rostrata*. Fibres were prepared from each species acclimated to normoxic water conditions, or following a 2 h, acute hypoxic exposure at levels representing 40% of each species' critical oxygen tension. Although mitochondrial respiratory fluxes for normoxia-acclimated animals were similar for both species, reactive species production in the epaulette shark was approximately half that of the shovelnose ray under normoxic conditions, even when normalised to tissue oxidative phosphorylation flux. The hypoxia-sensitive shovelnose ray halved oxidative phosphorylation flux and cytochrome *c* oxidase flux was depressed by 34% following hypoxic stress. In contrast, oxidative phosphorylation flux of the epaulette shark ventricular fibres isolated from acute hypoxia exposed the animals remained similar to those from normoxia-acclimated animals. However, uncoupling of respiration revealed depressed electron transport systems in both species following hypoxia exposure. Overall, the epaulette shark ventricular mitochondria showed greater oxidative phosphorylation stability and lower reactive species outputs with hypoxic exposure, and this may protect cardiac bioenergetic function in hypoxic tropical waters.

Keywords Mitochondria · Hypoxia tolerance · Shark

Abbreviations

CI	Complex I
CII	Complex II
CCO	Cytochrome *c* oxidase
ETS	Electron Transport System
OXP	Oxidative phosphorylation system
NO	Nitric oxide
RCR	Respiratory control ratio
RS	Reactive species
$\%RS/O_2$	The percentage of reactive species relative to oxygen consumed

Communicated by I.D. Hume.

A. J. R. Hickey (✉)
School of Biological Sciences, The University of Auckland, Auckland, New Zealand
e-mail: a.hickey@auckland.ac.nz

G. M. C. Renshaw
Hypoxia and Ischemia Research Unit, School of Physiotherapy and Exercise Science, Griffith University, Brisbane, QLD, Australia

B. Speers-Roesch · J. G. Richards · A. P. Farrell · C. J. Brauner
Department of Zoology, University of British Columbia, Vancouver, BC, Canada

Y. Wang
Department of Biology, Queens University, Kingston, ON, Canada

A. P. Farrell
Faculty of Land and Food Systems, University of British Columbia, Vancouver, BC, Canada

Introduction

Understanding hypoxic tolerance is fundamentally important in biomedical contexts of chronic coronary obstruction, transplant, trauma and invasive surgery. Hypoxia and ischemia not only starve tissues of oxygen and elevate metabolic waste products, they can also elevate oxidative stress with progressive hypoxia and upon reoxygenation (Wheaton and Chandel 2011; Murphy 2009). At normal mammalian temperatures hypoxic stress generally further enhances oxidative damage (de Groot and Rauen 2007), and in excess oxidative stress can trigger apoptosis and necrosis (Papaharalambus and Griendling 2007). Mitochondria appear to be acutely sensitive to hypoxic insults, and play significant roles in governing cell fates via apoptotic and necrotic pathways (Hand and Menze 2008).

In mammals, the heart is highly aerobic and hypoxia-sensitive organ with a three- to four-fold shorter extracorporeal survival time than the liver at 4°C (6 h heart, 18–20 h liver, Talbot and D'Alessandro 2009). However, some vertebrate species are adapted to tolerate extended periods of environmental hypoxia and provide potential models to better explore hypoxia tolerance (Hochachka and Lutz 2001). Indeed, in vivo measurements of cardiac performance in species such as crucian carp (*Carassius carassius*) (Stecyk et al. 2004) and freshwater turtles (e.g. *Chrysemys picta*) (Overgaard et al. 2007) show that the heart can continue to beat for days to months in complete anoxia, provided that temperatures are below 10°C (Glass et al. 1983; Overgaard et al. 2007). At higher temperatures, anoxia tolerance is greatly shortened in these species, to levels of hypoxia tolerance observed in other species (Overgaard et al. 2004, 2007). Therefore, non-mammalian vertebrates that show hypoxia tolerance at temperatures approaching those within mammals are of great interest.

The epaulette shark, *Hemiscyllum ocellatum*, is a small tropical Australasian elasmobranch (maximum length 107 cm) (Last and Stephens 1994) that can tolerate 3.5 h of exposure to extremely low experimental oxygen tensions at relatively high temperatures (1 kPa, 24°C) (Renshaw and Dyson 1999; Wise et al. 1998; Soederstroem et al. 1999). This degree of hypoxia tolerance is rare among elasmobranchs, which typically do not encounter hypoxia. The unusual hypoxia tolerance of the epaulette shark is thought to have evolved in conjunction with intermittent nocturnal hypoxic bouts on reef platforms at low tide, where oxygen levels can drop below 6 kPa (30% of air-saturated water) (Wise et al. 1998).

In mammals, hypoxic insult and reperfusion injury can result in depressed electron transport system (ETS) function (Talbot and D'Alessandro 2009), most often at complexes I and III and, once damaged or altered these complexes may further elevate the formation of superoxide ($O_2^{\cdot-}$) which is generally converted to hydrogen peroxide (H_2O_2) by superoxide dismutases (SOD). When H_2O_2 is not in excess, various peroxidases and catalase degrade this volatile molecule to water (Murphy 2009). Here we term these molecules as reactive species (RS) molecules that override the intrinsic RS defences or antioxidant systems.

Although much is known about the effects of hypoxia exposure on mitochondrial based reperfusion injury in mammals, studies examining whether mitochondrial properties differ between hypoxia-tolerant versus hypoxia-sensitive species are lacking. It could also be predicted that, from the whole-animal level, epaulette shark-heart mitochondria are potentially more stable in the face of low or variable oxygen and ATP levels, and/or that there is tighter control on RS production and defences.

We investigated mitochondrial respiration and net RS production in permeabilised heart ventricle fibres from elasmobranchs for the first time. We compared the epaulette shark to the shovelnose ray *Aptychotrema rostrata*, a hypoxia-sensitive elasmobranch that lives at a similar temperature and proximity, yet displays a greater sensitivity to hypoxic exposure. Indeed in this work we had to expose both species to different environmental oxygen levels (epaulette shark 2 kPa, shovelnose ray 3 kPa in order to achieve equivalent blood oxygenation levels (ca. 0.7 vol% in arterial blood), primarily due to the greater Hb-O_2 binding affinity in the epaulette shark (present authors, work in preparation). Here we test the hypotheses that ventricular mitochondrial respiration in the epaulette shark would be more tolerant to acute hypoxic insult, and that they would produce less RS in routine respiration states (e.g. phosphorylating) and following exposure to hypoxia. Hypoxic exposures were performed both in vivo and in vitro (i.e. within the fibre assay). We combined high-resolution oxygraphs with purpose-built fluorospectrometers that simultaneously measured respiration and RS production in permeabilised ventricle fibres. We used an enzyme-linked fluorophore to expose the fibres to a range of oxygen concentrations and hypoxia-relevant metabolites. We found contrasting net RS production capacities and mitochondrial stabilities.

Methods and materials

Animal acquisition and holding

Epaulette sharks and shovelnose rays of mixed sexes were supplied by Cairns Marine (Cairns, Australia) or Seafish Aquarium Life (Dunwich, Australia), respectively. The animals were collected under A1 level commercial harvest licences granted by the Department of Primary Industries

(Australia). Epaulette sharks were caught near Heron Island, Great Barrier Reef, and transported live to Cairns Marine and held unfed for 2 days before transport by air and automobile to Moreton Bay Research Station, Stradbroke Island. Shovelnose rays were caught in Moreton Bay, and held at Moreton Bay Research Station. Fish were held for at least 5 days prior to experiments in a 10,000 L recirculating seawater system maintained at 28°C. Fish were fed prawns and squid at 1–2% body mass every other day, and food was withheld 24 h prior to sampling.

Experimental treatments

The permeabilised ventricular fibre preparation (described below) was conducted in both species following exposure to normoxic water or to an acute, 2 h hypoxic exposure. Epaulette sharks (345 ± 54 g, mean ± SEM) and shovelnose rays (959 ± 108 g) were transferred from holding tanks to each of four fibreglass aquaria (~300 L, one species per tank) containing recirculating filtered seawater (28°C) and allowed to acclimate for 12 h.

For the acute hypoxia exposure, epaulette sharks and shovelnose rays were exposed to 2 kPa (10% air saturation) and 3 kPa (15%) air saturation, respectively. These oxygen levels result in similar arterial hypoxemia for each species (unpublished data) and represent 40% of each species' critical oxygen tension (P_{crit}). To induce hypoxia, N_2 was bubbled into the aquaria and once the desired oxygen tension was reached the aquaria were covered with plastic bubble wrap and the water oxygen tension was continuously monitored with a DO meter (Oxyguard probe (Mark IV, Point Four Systems, Richmond, BC, Canada). Water oxygen tension was maintained for 2 h at the desired level by adjusting the amount of water surface covered with bubble wrap. After 2 h exposure to hypoxia, fish were removed and euthanized (2 g L^{-1} benzocaine dissolved in 95% ethanol). This entire protocol was repeated daily to achieve a total sample size of 5–6 fish per species and per exposure. The normoxia treatment group was treated identically to the hypoxia treated group, except air was continuously bubbled into the chamber.

Fibre permeabilisation

Following removal of hearts 25 mg of myocardium was dissected immediately and placed into modified ice-cold relaxing solution (in mM, 10 Ca-EGTA buffer, 0.1 free calcium, 20 imidazole, 20 taurine, 700 Sucrose, 50 K-MES, 0.5 DTT, 6.56 $MgCl_2$, 5.77 ATP, 15 phosphocreatine at pH 7.1). Fibre bundles were teased from the spongy layer of ventricular tissues with sharp forceps to approximately 0.5 × 1 mm were then placed into 1 ml of fresh relaxing solution with 50 μg saponin, and agitated for 30 min at 4°C to permeabilize fibres (Veksler et al. 1987; Hilton et al. 2010). Saponin perforates the sarcolemma of cardiac muscle fibres by targeting cholesterol, leaving intracellular structures such as mitochondria intact, due to their low cholesterol content. Fibres were then washed three times for 10 min in ice-cold incubation assay medium (in mM, 0.5 EGTA, 3 $MgCl_2$, 60 K-lactobionate, 700 sucrose, 20 taurine, 10 KH_2PO_4, and 1 mg mL^{-1} BSA in 20 mM HEPES, pH 7.1 at 30°C). Fibre bundles were blot-dried on lint-free filter paper and approximately 7–12 mg was weighed out for use in respiration assays.

Respiratory flux in permeabilised ventricle fibres

A multiple substrate-inhibitor titration protocol (Fig. 1) was employed to best reflect substrates present in vivo, and to explore relative changes of the electron transport system (ETS) and phosphorylation system components (Gnaiger 2009). Complex I (CI) substrates (malate and pyruvate) were added in conjunction with the complex II (CII, and succinate dehydrogenase) substrate succinate. Excess pyruvate (10 mM) was added to ensure removal of oxaloacetate, which inhibits CII. Parallel electron input also served to elevate superoxide release from mitochondria (Zoccarato et al. 2007; Muller et al. 2008). Overall our approach maximised the data collected while minimising the number of fish sacrificed. Two OROBOROS® Oxygraph-2 K (Anton Paar, Graz, Austria) were employed for oxygraphy, and these incorporated in-house, purpose-built fluorospectrometers (discussed below). Respiratory measurements of permeabilised ventricle fibre bundles were performed at 28°C in a 2 ml chamber containing assay medium, with a starting oxygen concentration of 197.8 nmol O_2 per mL at 101.3 kPa barometric pressure (air saturation). Respiration was measured as weight-specific oxygen flux [pmol O_2 (s mg wet weight)$^{-1}$], by monitoring the decline in oxygen concentration over time using the DATLAB 4 analysis software. We note that assay media containing urea and trimethylamine oxide (TMAO) that approximated levels found in elasmobranchs was tested and found to be less suitable for RS determination.

For simultaneous RS detection superoxide dismutase (10 U), horseradish peroxidase (10 U), and Amplex Ultrared (50 μM final concentration, Molecular Probes Invitrogen) was added to each chamber. Oxygen was then added to chambers (~40 kPa) to ensure oxygen was not rate limiting (Gnaiger 2011). State two (leak) respiration was reached by the addition of the pyruvate (10 mM) and malate (5 mM). Excess ADP (1.25 mM) stimulated oxidative phosphorylation (OXP) respiration, and then succinate (10 mM) was added to provide a measure of parallel electron transport from CI and CII.

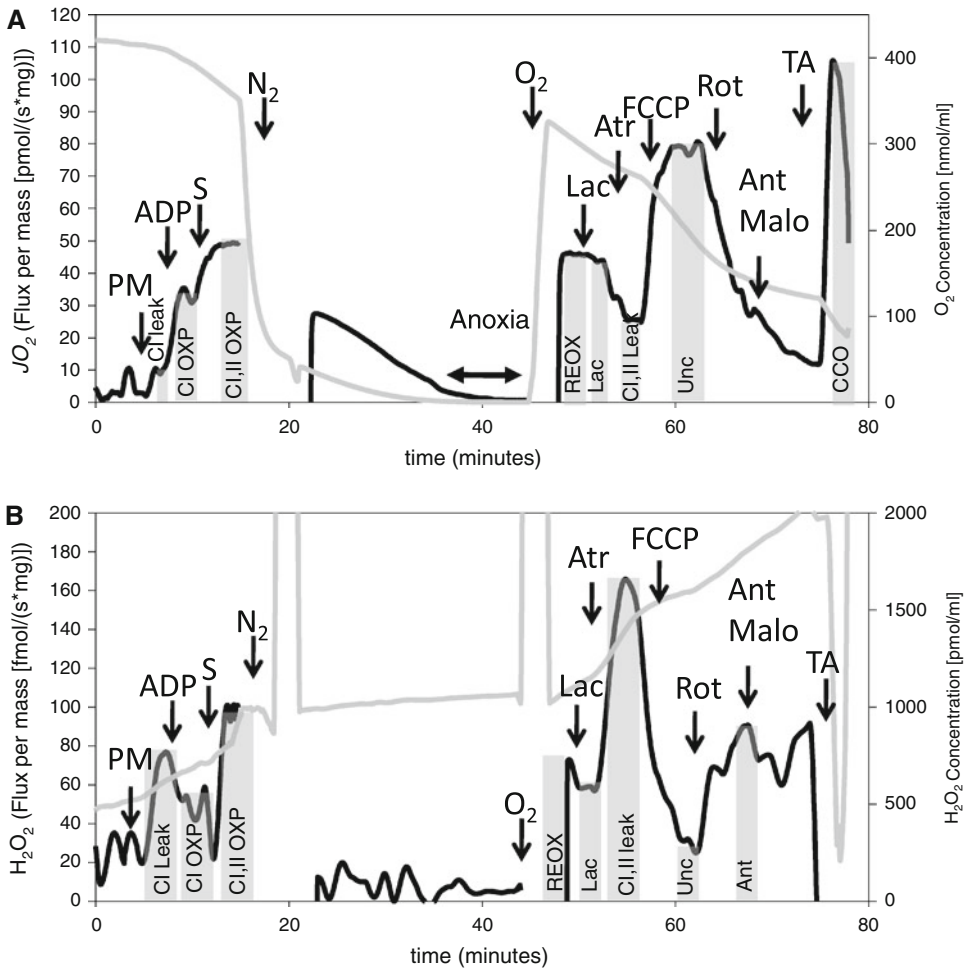

Fig. 1 Representative trace indicating substrate inhibitor protocol used for measurement of respiration flux (**a**) and reactive species(total) H_2O_2 production (**b**) in permeabilised ventricle fibres of the shovelnose ray (*Aptychotrema rostrata*). The substrate inhibitor titration protocol consisted of the addition of pyruvate and malate (PM), which supports Complex I flux in the leak state (CI Leak), followed by the addition of ADP and succinate (S) to drive oxidative phosphorylation (OXP) with parallel electron inputs through Complex I and II (CI, II OXP). Nitrogen was then introduced into the chamber which was then closed and anoxia was maintained for 10 min. Chambers where then re-oxygenated (REOX) and lactate (Lac) added to mimic lactate accumulation. Atractyloside (Atr) was added to measure post in vitro hypoxic exposure leak rates (CI, II Leak). Respiration was then uncoupled with FCCP (Unc) followed by CI inhibition with rotenone (Rot), and quenched with antimycin and malonate (Ant, Malo). *N*, *N*, *N*′, *N*′-tetramethyl-*p*-phenyldiamine (TMPD) and ascorbate (TA) was then added to determine maximal cytochrome *c* oxidase flux (chemical auto oxidation was determined and subtracted)

To test mitochondria tolerance to anoxia and reperfusion the chamber stoppers were opened and nitrogen was added to the header space to lower oxygen to approximately 3 kPa. Chambers were then closed and the fibres allowed to deplete oxygen and maintained in anoxia for 10 min. Oxygen was then reintroduced into the chambers and respiration allowed to recover. Given that lactate would most likely accumulate within anoxic myocytes, buffered lactate (10 mM, stock pH 7.0) was added to test for inhibition. Atractyloside (50 μM) was then added to determine leak respiration rates on combined CI and CII substrates and respiration was then uncoupled using serial injections of carbonyl cyanide *p*-(trifluoromethoxy) phenyl-hydrazone (FCCP, 0.5 μM) in order to maximise the flux through the ETS without the constraints of the phosphorylation system. Complex IV or cytochrome *c* oxidase (CCO) was then measured following the inhibition of C I, II and III with rotenone (1 μM), malonate (15 mM), and antimycin a (1 μM), respectively, and addition of the electron donor couple *N*, *N*, *N*′′, *N*′′-tetramethyl-*p*-phenylendiamine (TMPD, 0.5 μM) and ascorbate (2 μM). Chemical background for ascorbate and TMPD auto-oxidation was subtracted for each measurement.

Reactive species production in permeabilised ventricle fibres

RS was followed simultaneously with respirational flux using purpose-built fluorospectrometers. These utilised

light emitting diodes attached to fibre optic light guides to provide an excitation at 520 nm, and were placed adjacent to the viewing window of the Oroboros O2K oxygraph. Emitted light was then detected using a photodiode placed adjacent to the excitation fibre optic and covered with a 590 nm low pass filter. The voltage generated from the chamber fluorescence was stabilised by a loading, 20 mOhm resistor and the signal fed into the O2K pX meter. This amplified and integrated the RS signal with oxygen concentration and flux signals in DATLAB 4.3. To calibrate the fluorospectrometer, 400 pmol of resorufin, the final product of Amplex Ultrared, was added to each chamber prior to each assay. Steady state rates were followed using DATLAB 4.3 and corrected for tissue mass and background activities determined and subtracted prior to the addition of substrates. Four fluorospectrometers were used on two O2K oxygraphs. This permitted direct and simultaneous comparison of RS production rates in the same respiration states and conditions on fibre samples of both species.

Data analysis and statistics

Oxygraph data were analysed using Datlab 4.3 and Microsoft Excel. SPSS 16.0 was used to perform Students *t* tests directly where variances were equal. Data were transformed appropriately if variances differed significantly. An α value of 0.05 was chosen to represent statistically significant differences.

Results

Respiratory flux in permeabilised ventricle fibres

Few gross differences were apparent between the permeabilised ventricle fibres of the epaulette shark and shovelnose ray acclimated to normoxia. However, CCO flux was 37% higher in the shovelnose ray than the epaulette shark (Fig. 2, $P < 0.05$). The epaulette shark also showed a 36% ($P < 0.05$) greater flux when the ETS was uncoupled from OXP with FCCP (ETS/OXP-reox, Table 1) compared with the shovelnose ray. The epaulette shark also exhibited more than twice the ETS capacity relative to the leak respiration state when phosphorylation was inhibited by atractyloside (ETS/atr, $P < 0.05$, Table 1).

Normoxia-acclimated epaulette sharks showed lower relative leak rates, with higher respiratory control ratios (RCR, OXP relative to leak rates, Table 1) with either CI (RCR–CI), or CI and CII (RCR–CI + CII) substrates relative to the shovelnose ray. This suggests tighter coupling of the OXP system in the epaulette shark and/or a greater uncoupling in resting states in the shovelnose ray heart mitochondria.

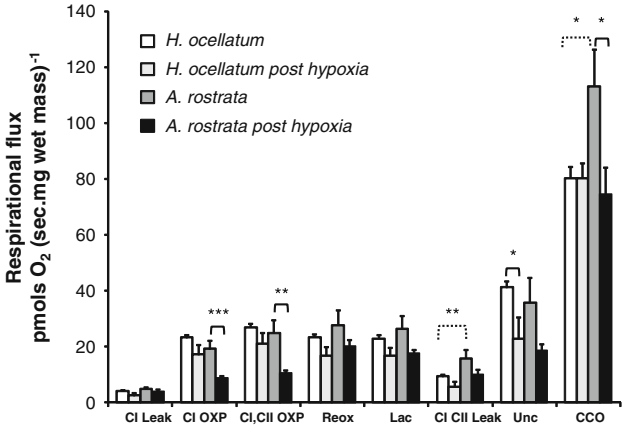

Fig. 2 Respirational flux in permeabilised ventricle fibres of the epaulette shark, the epaulette shark (*white*) and the shovelnose ray (*dark grey*) acclimated to normoxia or exposed to hypoxia. Only cytochrome *c* oxidase (CCO) flux differed between species prior to hypoxic exposure. Following a 2-h hypoxic exposure (epaulette shark *light grey*, 10% air saturation, and shovelnose ray *black*, 15% air saturation) the shovelnose ray showed depressed CI-OXP and CI, II OXP (refer to Fig. 1). Following reoxygenation (Reox) oxidative phosphorylation capacity returned in the shovelnose ray. Uncoupled respiration appeared to be depressed after exposure to hypoxia in vivo in the epaulette shark, while cytochrome *c* oxidase flux was depressed in CCO following hypoxic exposure in the shovelnose ray. *Dotted brackets* indicate statistically significant differences between species, while *solid brackets* indicate statistically significant differences within species following hypoxic exposure in vivo. Values represent mean ± standard error of the mean; *P* values: *0.05, **0.01, ***0.005. Refer to Fig. 1 legend for a description of *x* axis abbreviations and their association with the substrate inhibitor titration protocol

Following exposure to hypoxia in vivo, the permeabilised ventricle fibres of shovelnose ray exhibited a 54% ($P < 0.05$) depression in CI OXP flux, a 58% ($P > 0.05$) depression in CI + CII OXP flux and a 33% decrease in CCO flux ($P < 0.05$) relative to normoxia-acclimated animals (Fig. 2). These same parameters for epaulette sharks exposed to hypoxia in vivo did not differ significantly from normoxia-acclimated epaulette sharks. However, hypoxic exposure did decrease ETS respirational flux of the epaulette shark relative to normoxia-acclimated animals ($P < 0.05$), while no difference was observed for the shovelnose ray (Table 1). CCO remained relatively intact in the epaulette shark following hypoxic exposure, while the shovelnose ray showed a 33% depression in flux ($P < 0.05$) relative to normoxic controls.

Following exposure to hypoxia in vivo, the RCR–CI for the shovelnose rays decreased by almost 50% relative to that of the normoxia-acclimated shovelnose rays. For epaulette sharks, the RCR–CI remained high following in vivo hypoxic exposure. Following the within assay anoxic and reoxygenation exposure the OXP flux of shovelnose rays returned to rates similar to those in untreated shovelnose rays (Fig. 2, $P < 0.005$). Finally, a decrease in the

Table 1 Mitochondrial respirational flux following exposure to various substrates and inhibitors in isolated permeabilised ventricle fibres from the epaulette shark (*Hemiscyllum ocellatum*) and the shovelnose ray (*Aptychotrema rostrata*) acclimated to normoxia or hypoxia

	RCR CI	RCR CI + II	ETS/OXP-reox	ETS/atr	%CI of OXP	OXP_{-reox}/OXP
Normoxia						
Epaulette shark ($n = 6$)	6.8 ± 1.1	2.8 ± 0.4	1.7 ± 0.1	4.9 ± 0.8	17.9 ± 2.6	0.92 ± 0.10
Shovelnose ray ($n = 6$)	$4.0 \pm 0.3^{+}$	$1.7 \pm 0.1^{++}$	1.3 ± 0.1+	$2.2 \pm 0.2^{+++}$	24.4 ± 1.8^{ns}	1.13 ± 0.12^{ns}
Hypoxia						
Epaulette shark ($n = 6$)	7.7 ± 1.1^{ns}	3.1 ± 0.3^{ns}	1.4 ± 0.1*	4.2 ± 0.2^{ns}	18.3 ± 2.6^{ns}	0.80 ± 0.03^{ns}
Shovelnose ray ($n = 5$)	2.2 ± 0.1****	1.8 ± 0.2^{ns}	1.0 ± 0.1^{ns}	1.9 ± 0.2^{ns}	16.1 ± 2.6*	1.9 ± 0.2***

RCR CI represents the respiratory control ratios determined with complex 1 (CI) substrates pyruvate (10 mM) and malate (5 mM) with and without 1.25 mM ADP. The RCR CI + CII values were determined with pyruvate, malate and the complex II (CII) substrate succinate (10 mM) and in the presence of atractyloside. ETS/OXP-reox refers to the ratio of respirational flux in the uncoupled state following addition of FCCP, relative to the coupled phosphorylating state determined after reoxygenation. The ETS/atr ratio provides an additional measure of ETS capacity relative to the leak respiration state when phosphorylation is inhibited by atractyloside. %CI of OXP refers to the contribution of CI derived flux to overall OXP and OXP_{-reox}/OXP compares the respirational fluxes prior to and after anoxia and reoxygenation. The symbol "+" indicates statistically significant differences for comparisons between species in normoxia, while "*" indicates statistically significant differences between comparisons of hypoxia and normoxia within a species where^{+} ,* refers to 0.05, $^{++}$,** refers to 0.01, $^{+++}$,*** refers to 0.005 and **** refers to <0.001. Values represent mean ± standard errors

relative contribution of CI to combined CI and CII OXP flux was apparent in hypoxic versus normoxic-exposed shovelnose rays (Table 1, $P < 0.01$), and this suggests a loss of CI function during OXP. The percentage of CI was unchanged in epaulette sharks.

Reactive species production in permeabilised ventricle fibres

Depending upon respiration state, the RS production per unit mass of permeabilised ventricle fibres was 50–80% lower in normoxic-acclimated epaulette sharks than in shovelnose rays (Fig. 3). Following exposure to hypoxia in vivo, there was a substantial decrease in permeabilised ventricle fibre RS production in shovelnose rays under almost every condition (Fig. 3). There were no significant differences in epaulette sharks with the exception of Complex I fuelled oxidative phosphorylation (CI OXP). The greatest difference in permeabilised ventricle fibre RS production was observed between species following reoxygenation (Reox) and after the introduction of lactate (Lac) in the non-phosphorylating state (Fig. 3). RS production from permeabilised fibres increased substantially in both species with the addition of atractyloside, which inhibits phosphorylation (CI + II Leak). Importantly, this indicates that the mitochondria of epaulette sharks have the potential to produce RS at a similar rate to that of shovelnose rays, which was also observed following antimycin addition. Notably, following uncoupling with FCCP, RS production still remained lower in epaulette shark mitochondria than for shovelnose ray mitochondria even after exposure to hypoxia in vivo.

When RS production is expressed as a percentage of oxygen consumed (%RS/O_2) it is apparent that mitochondrial

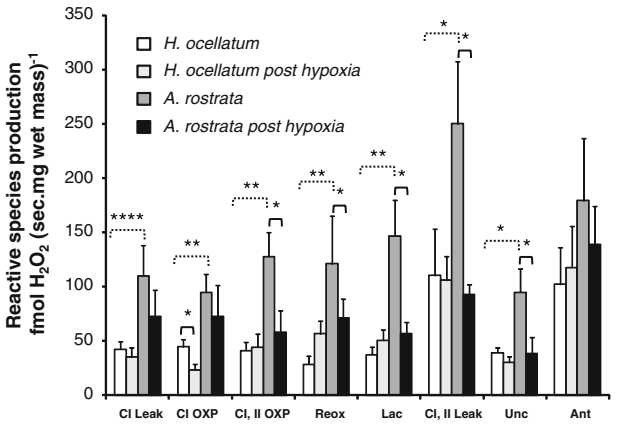

Fig. 3 Reactive species (RS) production by in permeabilised ventricle fibres form the epaulette shark (*white*) and the shovelnose ray (*dark grey*), acclimated to normoxia or exposed to hypoxia. RS production was coupled to the production of H_2O_2 using superoxide dismutase and determined in different respiration states (as outlined in Fig. 1). In most cases, RS production in animals sampled in normoxia was elevated in the shovelnose ray relative to that in the epaulette shark. Following in vivo exposure to hypoxia RS production remained similar in the epaulette shark (*light grey*) while it decreased markedly in most cases for the shovelnose ray (*black*). Refer to Fig. 1 legend for a description of *x* axis abbreviations and their association with the substrate inhibitor titration protocol

RS production in the non-phosphorylating/leak state is similar across species exposed to normoxia (Fig. 4). Notably, %RS/O_2 rapidly declines with the addition of ADP from 1.5 and 2.1%, to 0.2 and 0.5%, in the epaulette shark and shovelnose ray, respectively. This decrease in RS/O_2 was more substantial in epaulette sharks (~80%) than in shovelnose rays (60%), and overall epaulette sharks produce approximately 60–70% less RS/O_2 than shovelnose rays when mitochondria are phosphorylating or uncoupled, and

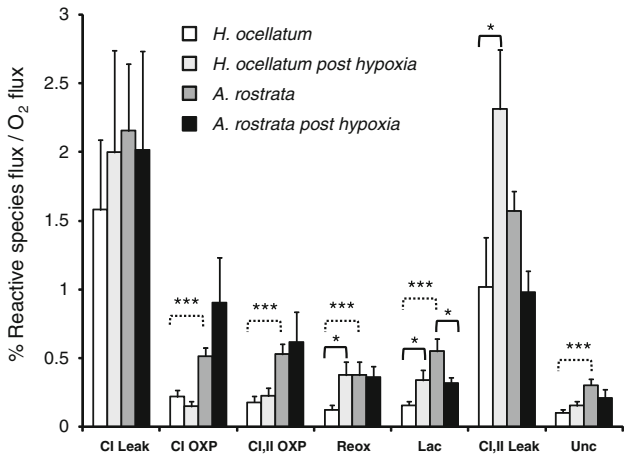

Fig. 4 Reactive species (RS) production expressed as a percentage of respirational flux in permeabilised ventricle fibres from the epaulette shark (*white*) and the shovelnose ray (*dark grey*) acclimated to normoxia or exposed to hypoxia. The %RS production of O_2 indicates that the relative efficiency of RS production declines as respiration accelerates. In the Leak states the % H_2O_2/O_2 is similar for both species, yet with phosphorylation (CI OXP, CI, II OXP) the epaulette shark produces less $\%H_2O_2/O_2$. Following in vivo hypoxic stress, the $\%H_2O_2/O_2$ remained similar for the epaulette shark (*pale grey*), except following reoxygenation after in vitro anoxic exposure (Reox, Lac). With blockade of phosphorylation by atractyloside (CI, II Leak) the epaulette shark was also sensitised following in vivo hypoxic exposure. The shovelnose ray (*black*) retained high $\%H_2O_2/O_2$ values after in vivo hypoxic exposure, apart from in the presence of lactate and atractyloside. Refer to Fig. 1 legend for a description of *x* axis abbreviations and their association with the substrate inhibitor titration protocol

indicate that proportionately fewer electrons are lost from the ETS as RS in the epaulette shark.

Following in vivo hypoxic exposure, CI substrate fuelled OXP RS/O_2 ratios approached 1% of oxygen consumed for shovelnose rays. Note that this is similar for epaulette shark ventricular fibres in the presence of atractyloside. Although fibres from the epaulette shark exposed to hypoxia elevate $\%RS/O_2$ following in vitro anoxia/reoxygenation, these values remained similar to the higher phosphorylating values for shovelnose rays. On addition of atractyloside, epaulette sharks showed an increase in the $\%RS/O_2$, which again indicates that this species has a similar net capacity to release RS as shovelnose rays.

Discussion

Compared with the hypoxia-sensitive shovelnose rays, the hypoxia-tolerant epaulette shark showed differences in heart mitochondrial function on several fronts, all of which are consistent with the heart having a greater tolerance to stresses associated with hypoxia. Mitochondrial respiration appears to be more resistant to in vivo hypoxia in epaulette sharks than in shovelnose rays. In general, when fibres were harvested from fish that had experienced an acute hypoxic exposure, the epaulette shark produced only one-half to one-quarter the RS of those from shovelnose rays whether exposed to hypoxia or not. This was also true when RS production was expressed as a percentage of oxygen consumption, as prior to hypoxia exposure in vivo, mitochondria from epaulette sharks produced only 28–40% of the RS relative to shovelnose rays in OXP. These findings are consistent with our predictions that the hypoxia-tolerant epaulette shark would possess traits of mitochondrial function and stability that facilitate resistance to hypoxic stress. Perhaps more fundamentally, these data also provide clear evidence that mitochondria differ among species, and these differences are concordant with species ecological requirements.

The greater resistance of mitochondrial function to in vivo hypoxia exposure in the epaulette shark is all the more impressive when one considers that this species was exposed to a more severe hypoxia (2 kPa oxygen) than the shovelnose ray (3 kPa oxygen). These oxygen tensions represent 40% of each species' critical oxygen tension (present authors, unpublished results). This is the environmental oxygen tension at which oxygen consumption rate transitions from being independent of environmental oxygen, to being absolutely dependent on environmental oxygen. We chose to expose both species to these different levels of environmental oxygen in order to account for the greater Hb-O_2 binding affinity in the epaulette shark relative to the shovelnose ray (present authors, work in preparation). Under these conditions, both species experienced similar arterial oxygen levels (approximately 0.7 vol% in arterial blood) during 2 h acute hypoxia exposure.

Simple comparison of mitochondrial respiration rates for animals held under normoxic conditions shows that both species have similar overall capacities in terms of OXP flux. However, some differences were apparent. The shovelnose ray displayed a greater CCO flux and had lower RCRs than the epaulette shark (RCR–C1 and RCR–CI + CII, Table 1). Mitochondria of the epaulette shark also display a 36% greater apparent ETS reserve capacity relative to that of shovelnose rays.

Cytochrome *c* oxidase

Elevated CCO in the shovelnose ray is contrary to predictions. CCO binds oxygen and generally appears to be in excess capacity relative to ETS flux in most mitochondria (Gnaiger et al. 1998b), and several explanations for this excess CCO flux capacity have been proposed (Gnaiger et al. 1998a). Mammalian cardiac mitochondria also show a higher CCO flux capacity relative to tissues such as liver (Benard et al. 2006; Gnaiger et al. 1998b). This higher

relative flux of CCO can result from elevated CCO amounts, or from altered kinetics, i.e. higher affinities for substrates (O_2, cytochrome *c*) (Gnaiger et al. 1998a), and an elevated CCO flux should improve O_2 binding at low oxygen tensions (Gnaiger 2003). One would therefore expect that the epaulette shark would have a higher CCO flux than the shovelnose ray. These data also differ from those observed in a study of blennioid teleosts, where elevated CCO occurred in more hypoxia-tolerant and thermostable rockpool species (Hilton et al. 2010).

In mammals CCO is inhibited by the cardiac vasodilator nitric oxide (NO) (Antunes et al. 2004; Paulus and Bronzwaer 2004; Davidson and Duchen 2006). The NO system can become dysfunctional in pathological settings, including following ischemia (Borutaite et al. 2001; Davidson and Duchen 2006). Elevated or reserve capacities of CCO should promote O_2 binding at low oxygen tensions and/or lessen the impacts of NO inhibition. Although these data conflict with expectations, we note that both species have high ventricular CCO/ETS ratios (3.0–4.5) relative to mammals (2.3) assayed under similar conditions (Hickey et al. 2009).

CCO is more stable in the epaulette shark, as CCO flux remained constant while it decreased in shovelnose rays following hypoxic exposure. This is consistent with an increased tolerance to oxidative stress. CCO is, in part, functionally dependent on cardiolipin in the inner mitochondrial membrane (Zhong et al. 2004; Chicco and Sparagna 2006; Chen and Lesnefsky 2006), and cardiolipin is prone to oxidative damage from RS, which also affects CCO flux (Chicco and Sparagna 2006; Chen and Lesnefsky 2006). The greater stability of the epaulette shark CCO flux to hypoxia is either greater than that of the shovelnose ray and/or there is less exposure of the epaulette shark CCO molecules to RS.

Coupled and uncoupled respiration

The naturally hypoxia-tolerant epaulette shark shows less inhibition of mitochondrial function following hypoxic exposure in vivo, while the shovelnose ray shows depression in OXP. Surprisingly, respiration returned to normoxic levels after in vitro anoxic exposure and reoxygenation in the shovelnose ray. This return of OXP capacity was unexpected. Pre-conditioning of tissues is a common procedure in transplant and major surgical interventions, and involves ischemic bouts that may be applied directly to the organ (by clamping arterial supplies) or even by obstruction of blood flow in a limb that is distal to the target organ (Schneeberger et al. 2008; Gomez et al. 2009). This procedure may benefit tissues by enhancing cardiomyocyte glycolytic capacities and reserves (Zuurbier et al. 2009) and decreasing mitochondrial RS production and mitochondrial membrane permeability transition pore opening (Halestrap et al. 2007). An unexplained phenomenon of post-conditioning has also recently become apparent, where brief post-transplant ischemic bouts by clamping arterial vessels improves graft function (Kaur et al. 2009). The restoration of respirational flux in the shovelnose ray following in vitro anoxic exposure may provide a preliminary insight to the underlying mechanisms of post-conditioning.

The RCR ratios (RCR–CI and RCR–CI + CII, Table 1) for the epaulette shark were substantially higher than for the shovelnose ray (Table 1). The RCR is often used as an indicator of leak rate, or coupling efficiency of the ETS to the OXP system (Rolfe and Brown 1997). Elevation of the leak state requires greater inner membrane proton permeability. The assumed net result is that while electron flux through the ETS may be rapid, fewer protons from the intermembrane space pass through the F_1/F_0 ATP synthase under phosphorylating states (Rolfe and Brown 1997). Phosphorylation efficiency may be dynamic however, as even apparently uncoupled mitochondria may still show good coupling based upon PO ratios (the amount of ATP made for a given amount of molecular oxygen) (Rolfe and Brown 1997). Therefore, although the lower RCRs of the shovelnose ray may not entirely reflect OXP efficiency, these data do show that the epaulette shark mitochondrial phosphorylation systems exert greater control over respiration than those of the shovelnose ray.

Reactive species production

Elevated leak has been linked to lowered RS production (Murphy 2009; Rolfe and Brown 1997) and, therefore, the shovelnose ray should show lower RS outputs. High membrane potentials maintain the ETS complexes in a more reduced state and this promotes RS production from ETS Complexes I and III (Murphy 2009; Rolfe and Brown 1997). However, the epaulette shark shows high RCRs, yet lower RS outputs than the shovelnose ray (Fig. 3). The epaulette shark also shows lower RS relative to oxygen turnover (Fig. 4). Importantly, both elasmobranch species have similar $\%RS/O_2$ when mitochondria are in non-phosphorylating coupled states. The similar relative RS outputs from non-phosphorylating mitochondria also show that the lower RS production in phosphorylating states is not an artefact and that when artificially inhibited, epaulette sharks retain the mechanism by which to release RS.

Our data show that RS production is dependent on phosphorylation state, and activation of phosphorylation in the epaulette shark produces less than half the RS per molecule of oxygen than the shovelnose ray. Although this is known, RS is generally measured in ADP starved states,

or in the presence of inhibitors such as antimycin and rotenone with single substrates such as succinate. These states never occur in vivo. Few measure RS production in actively phosphorylating mitochondria with multiple substrates (Hickey et al. 2009; Zoccarato et al. 2007; Muller et al. 2008). Importantly the measurement of RS relative to OXP flux is crucial to understanding the actual RS outputs, as mitochondria, in particular those of the hypoxic heart, are never absolutely starved of ADP (Loiselle 1985), indeed one would predict regionally increased [ADP] in hypoxia. Moreover, if RS was determined only in inhibited states, RS outputs of both species studied here would appear similar and therefore no difference in net RS production would be evident. Taken together, these data show that the epaulette shark not only releases less potentially damaging RS, but also has more efficient mitochondria as fewer electrons are lost to RS than in the shovelnose ray, and these may contribute to ATP production.

The lower CI-mediated RS production of the epaulette shark-heart mitochondria may in part explain the tolerance of this species to endure regular bouts of hypoxia. Notably, the shovelnose ray displayed an elevation in the CI-mediated $\%RS/O_2$ following in vivo hypoxia exposure, while the epaulette shark did not. The post-hypoxia OXP data show that the epaulette shark has more robust mitochondria and that this potentially results from a lower general RS output. CI-dependent OXP was also more robust to hypoxia exposure in the epaulette shark, and we note that CI can be a source of superoxide in mammalian and avian systems (Murphy 2009; Barja and Herrero 1998). CI also appears to be susceptible to RS damage (Murphy 2009; Papa et al. 2008) and CI activity is often depressed following ischemic insults (Lesnefsky et al. 2001). The epaulette shark shows a greater uncoupling effect following FCCP addition, and indicates a greater ETS reserve capacity relative to the shovelnose ray. This may serve two roles: (1) a greater ETS reserve may permit increased loading within the ETS (i.e. that electrons are held and not released as superoxide), or (2) an excess ETS capacity may permit the sacrificial loss of ETS complexes. Notably, OXP remained similar between normoxia- and hypoxia-exposed epaulette sharks, while the uncoupled flux relative to coupled flux (ETS/coup, Table 1) dropped in epaulette sharks. This indicates a functional loss of the ETS following hypoxic stress. It is of note that specific subunits of CI are turned over almost hourly in mammalian mitochondria, and impairment of this energy-dependent replacement (such as during hypoxia) compromises respiration (Papa et al. 2008). The epaulette shark mitochondria are therefore not immune to hypoxic insults, but they are perhaps more efficient and better defended against hypoxic insult than those of the shovelnose ray, so that they can at least maintain OXP function.

Conclusions

The impressive hypoxia tolerance of the epaulette shark at warm temperatures was reflected by the greater integrity and stability of its ventricular mitochondria during hypoxic insult relative to the shovelnose ray. The ability to maintain OXP capacity in assays following in vivo hypoxia, as well as with anoxia during the in vitro assay, is perhaps most important. The maintenance of mitochondrial efficiency (RCR ratios) with low levels of RS production perhaps suggests that less damage occurs in the face of an ischemia and reperfusion. This then ensures resumption of adequate and efficient ATP generation on reoxygenation. A greater resilience of OXP function in the heart mitochondria of the epaulette shark will also aid energy-dependent restoration of depleted antioxidant defences on entry to, and following hypoxic insults. The depression in $\%RS/O_2$ may also result from greater ETS efficiencies and capacities, and this may also provide increased OXP efficiency and reserves in the epaulette shark mitochondria. Decreased RS production, with increased ETS reserve may further defend epaulette shark-heart function, as excessive RS can trigger apoptosis, while ATP depletion triggers necrosis (Hand and Menze 2008). We note clear species' differences in mitochondrial function are apparent, and that these differences are mostly consistent with adaptations for hypoxia tolerance in epaulette sharks. However, we note that additional species need to be studied in order to conclusively classify these species differences as adaptive. Perhaps most importantly, the epaulette shark maintains stable heart mitochondria in the face of hypoxia at 28°C. The underlying mechanism for this is of immediate biomedical relevance.

Acknowledgments This research was supported by Natural Science and Engineering Research Council Discovery grants to JGR, YW, APF and CJB. CJB was supported by a Killam Faculty Research Fellowship. AJRH was supported by the University of Auckland Early Career Excellence Award. BS-R was supported by a Journal of Experimental Biology Travelling Fellowship from the Company of Biologists, a Comparative Physiology and Biochemistry Student Research Grant from the Canadian Society of Zoologists, and a Graduate Travel Award from the Department of Zoology, University of British Columbia. We thank Kevin and Kathy Townsend at the Moreton Bay Research Station for all their efforts during our stay.

References

Antunes F, Boveris A, Cadenas E (2004) On the mechanism and biology of cytochrome oxidase inhibition by nitric oxide. Proc Natl Acad Sci USA 101:16774–16779. doi:10.1073/pnas.0405368101

Barja G, Herrero A (1998) Localization at Complex I and mechanism of the higher free radical production of brain non-synaptic mitochondria in the short-lived rat than in the longevous pigeon. J Bioenerg Biomembr 30:235–243

Benard G, Faustin B, Passerieux E, Galinier A, Rocher C, Bellance N, Delage J-P, Casteilla L, Letellier T, Rossignol R (2006) Physiological diversity of mitochondrial oxidative phosphorylation. Am J Physiol 291C:1172–1182

Borutaite V, Matthias A, Harris H, Moncada S, Brown G (2001) Reversible inhibition of cellular respiration by nitric oxide in vascular inflammation. Am J Physiol 281:H2256–H2260

Chen Q, Lesnefsky EJ (2006) Depletion of cardiolipin and cytochrome c during ischemia increases hydrogen peroxide production from the electron transport chain. Free Rad Biol Med 40:976–982

Chicco AJ, Sparagna GC (2006) Role of cardiolipin alterations in mitochondrial dysfunction and disease. Am J Physiol Cell Physiol 292:C33–C44

Davidson SM, Duchen MR (2006) Effects of NO on mitochondrial function in cardiomyocytes: pathophysiological relevance. Cardiovasc Res 71:10–21

de Groot H, Rauen U (2007) Ischemia-reperfusion injury: processes in pathogenetic networks: a review. Transpl Proc 39:481–484

Glass ML, Boutilier RG, Heisler N (1983) Ventilatory control of arterial PO2 in the turtle *Chrysemys picta bellii*: Effects of temperature and hypoxia. J Comp Physiol B Biochemi Syst Environ Physiol 151:145–153

Gnaiger E (2003) Oxygen conformity of cellular respiration; a perspective of mitochondrial physiology. Through the lifecycle. Kluwer Academic/Plenum Publishers, New York

Gnaiger E (2009) Capacity of oxidative phosphorylation in human skeletal muscle: New perspectives of mitochondrial physiology. Int J Biochem Cell Biol 41:1837–1845

Gnaiger E (2011) Capacity of oxidative phosphorylation in human skeletal muscle. New perspectives of mitochondrial physiology. Int J Biochem Cell Biol (in press)

Gnaiger E, Lassnig B, Kuznetsov A, Rieger G, Margreiter R (1998a) Mitochondrial oxygen affinity, respiratory flux control and excess capacity of cytochrome *c* oxidase. J Exp Biol 201:1129–1139

Gnaiger E, Lassnig B, Kuznetsov AV, Rieger G, Raimund M (1998b) Mitochondrial oxygen affinity, respiratory flux control and excess capacity of cytochrome *c* oxidase. J Exp Biol 201:1129–1139

Gomez L, Li B, Mewton N, Sanchez I, Piot C, Elbaz M, Ovize M (2009) Inhibition of mitochondrial permeability transition pore opening: translation to patients. Cardiovasc Res 83:226–233

Halestrap AP, Clarke SJ, Khaliulin I (2007) The role of mitochondria in protection of the heart by preconditioning. Biochim Biophys Acta (BBA) Bioenergetics 1767:1007–1031

Hand SC, Menze MA (2008) Mitochondria in energy-limited states: mechanisms that blunt the signaling of cell death. J Exp Biol 211:1829–1840

Hickey AJR, Chai CC, Choong SY, de Freitas Costa S, Skea GL, Phillips ARJ, Cooper GJS (2009) Impaired ATP turnover and ADP supply depress cardiac mitochondrial respiration and elevate superoxide in non-failing spontaneously hypertensive rat hearts. Am J Physiol Cell Physiol 297:C766–C774

Hilton Z, Clements K, Hickey A (2010) Temperature sensitivity of cardiac mitochondria in intertidal and subtidal triplefin fishes. J Comp Physiol B Biochem Syst Environ Physiol 180:1–12

Hochachka PW, Lutz PL (2001) Mechanism, origin and evolution of anoxia tolerance in animals. Comp Biochem Physiol B 130:435–459

Kaur S, Jaggi AS, Singh N (2009) Molecular aspects of ischaemic post-conditioning. Fund Clin Pharm 23:521–536

Last PR, Stephens JD (1994) Sharks and rays of Australia. CSIRO, Australia

Lesnefsky EJ, Moghaddas S, Tandler B, Kerner J, Hoppel CL (2001) Mitochondrial dysfunction in cardiac disease: ischemia–reperfusion, aging, and heart failure. J Mol Cell Cardiol 33:1065–1089

Loiselle DS (1985) The rate of resting heat production of rat papillary muscle. Pflugers Arch 405:155–162

Muller FL, Liu Y, Abdul-Ghani MA, Lustgarten MS, Bhattacharya A, Jang Y, Van Remmen H (2008) High superoxide production in skeletal-muscle mitochondria respiring on both complex I and complex II substrates. Biochem J 409:491–499

Murphy MP (2009) How mitochondria produce reactive oxygen species. Biochem J 417:1–13

Overgaard J, Gesser H, Wang T (2007) Tribute to P. L. Lutz: cardiac performance and cardiovascular regulation during anoxia/hypoxia in freshwater turtles. J Exp Biol 210:1687–1699

Overgaard J, Stecyk JAW, Gesser H, Wang T, Farrell AP (2004) Effects of temperature and anoxia upon the performance of in situ perfused trout hearts. J Exp Biol:655–665

Papa S, De Rasmo D, Scacco S, Signorile A, Technikova-Dobrova Z, Palmisano G, Sardanelli AM, Papa F, Panelli D, Scaringi R, Santeramo A (2008) Mammalian complex I: a regulable and vulnerable pacemaker in mitochondrial respiratory function. Biochim Biophys Acta (BBA) Bioenergetics 1777:719–728

Papaharalambus CA, Griendling KK (2007) Basic mechanisms of oxidative stress and reactive oxygen species in cardiovascular injury. Trends Cardiovasc Med 17(2):48–54

Paulus WJ, Bronzwaer JGF (2004) Nitric oxide's role in the heart: control of beating or breathing? Am J Physiol Heart Circ Physiol 287:H8–H13

Renshaw GMC, Dyson SE (1999) Increased nitric oxide synthase in the vasculature of the epaulette shark brain following hypoxia. Neurochem 10(8):1707–1712

Rolfe DF, Brown GC (1997) Cellular energy utilization and molecular origin of standard metabolic rate in mammals. Physiol Rev 77:731–758

Schneeberger S, Kuznetsov AV, Seiler R, Renz O, Meusburger H, Mark W, Brandacher G, Margreiter R, Gnaiger E (2008) Mitochondrial ischemia-reperfusion injury of the transplanted rat heart: improved protection by preservation versus cardioplegic solutions. Shock 30:365–371

Soederstroem V, Renshaw GMC, Nilsson GE (1999) Brain blood flow and blood pressure during hypoxia in the epaulette shark *Hemisyllium ocellatum*, a hypoxia-tolerant elasmobranch. J Exp Biol 202:829–835

Stecyk JAW, StenslÃ¸kken Kr-O, Farrell AP, Nilsson GrE (2004) Maintained cardiac pumping in anoxic crucian carp. Science 306:77

Talbot D, D'Alessandro AM (eds) (2009) Organ donation and transplantation after cardiac death. Oxford Press Inc., New York

Veksler VI, Kuznetsov AV, Sharov VG, Kapelko VI, Saks VA (1987) Mitochondrial respiratory parameters in cardiac tissue: a novel method of assessment by using saponin-skinned fibers. Biochim Biophys Acta 892:191–196

Wheaton WW, Chandel NS (2011) Hypoxia. 2. Hypoxia regulates cellular metabolism. Am J Physiol Cell Physiol 300:C385–C393

Wise G, Mulvey JM, Renshaw GMC (1998) Hypoxia tolerance in the epaulette shark (*Hemiscyllium ocellatum*). J Exp Biol 281:1–5

Zhong Q, Gohil VM, Ma L, Greenberg ML (2004) Absence of cardiolipin results in temperature sensitivity, respiratory defects, and mitochondrial DNA instability independent of pet56. J Biol Chem 279:32294–32300

Zoccarato F, Cavallini L, Bortolami S, Alexandre A (2007) Succinate modulation of H2O2 release at NADH:ubiquinone oxidoreductase (Complex I) in brain mitochondria. Biochem J 406:125–129

Zuurbier C, Smeele K, Eerbeek O (2009) Mitochondrial hexokinase and cardioprotection of the intact heart. J Bioenerg Biomembr 41:181–185